Charge-Separation Dynamics in Inorganic-Organic Ternary Blends for Efficient Infrared Photodiodes

Jarzab, Dorota; Szendrei, Krisztina; Yarema, Maksym; Pichler, Stefan; Heiss, Wolfgang; Loi, Maria A.

Published in:
Advanced Functional Materials

DOI:
10.1002/adfm.201001999

Publication date:
2011

FULL PAPER

Charge-Separation Dynamics in Inorganic–Organic Ternary Blends for Efficient Infrared Photodiodes

*Dorota Jarzab, Krisztina Szendrei, Maksym Yarema, Stefan Pichler, Wolfgang Heiss, and Maria A. Loi**

Knowledge about the working mechanism of the PbS:P3HT:PCBM [P3HT=poly(3-hexylthiophene), PCBM=[6,6]-phenyl-C_{61} -butyric acid methyl ester] hybrid blend used for efficient near-infrared photodiodes is obtained from time-resolved photoluminescence (PL) studies. To understand the role of each component in the heterojunction, the PL dynamics of the ternary (PbS:P3HT:PCBM) blend and the binary (PbS:P3HT, PbS:PCBM and P3HT:PCBM) blends are compared with the PL of the pristine PbS nanocrystals (NCs) and P3HT. In the ternary blend the efficiency of the charge transfer is significantly enhanced compared to the one of PbS:P3HT and PbS:PCBM blends, indicating that both hole and electron transfer from excited NCs to the polymer and fullerene occur. The hole transfer towards the P3HT determines the equilibration of their population in the NCs after the electron transfer towards PCBM, allowing their re-excitation and new charge transfer process.

1. Introduction

Solution-processed inorganic–organic hybrid devices are among the most promising low-cost alternatives to epitaxially grown, purely inorganic electronics. In these hybrid devices the active layer is a mixture of inorganic and organic semiconductors that are often themselves blends of colloidal inorganic nanocrystals (NCs) and organic molecules.[1–4] Although fabrication of this kind of heterostructure is rather challenging, in the past several groups have reported the successful application of binary inorganic–organic heterojunctions consisting of NCs and organic semiconductors for light-emitting diodes,[2,5] solar cells,[1] and near-infrared (NIR) photodetectors.[3,6,7] In these hybrid thin films, in general the NCs operate as sensitizers while the organic components serve as functional interfaces to extract carriers[8] or energy[9] from the nanocrystals.[3,4] While originally binary organic–inorganic blends were utilized, more recently, ternary blends of inorganic NCs and two different organic materials have also attracted researchers' attention.[4,10–13]

As a highlight of this approach, T. Rauch et al.[4] reported solution-processed, high performing, inorganic–organic hybrid photodiodes for infrared imaging. These photodiodes, composed of a combination of NIR-sensitive NCs (PbS) with a polymer/fullerene blend, show outstanding detection characteristics such as a responsivity of 0.5 AW^{-1} and detectivity of 2.3×10^9 Jones in the NIR spectral range. Interestingly, this high photosensitivity in the IR is obtained only for the ternary blend, whereas the external quantum efficiency of all binary reference samples is lower by more than one order of magnitude. This high sensitivity was attributed to ambipolar transport in the organic constituents, which follows a charge-transfer process from the NC to the organic species. However, no details were given of how this charge transfer should take place. Any further development of similar hybrid devices will require a deeper understanding of the underlying processes, such as charge separation and charge transfer between the inorganic and organic components in these ternary hybrids.

In this study, we investigated the operation principle of identical hybrid ternary blends, as used for the fabrication of the infrared imager.[4] The blend contains PbS-NCs as the inorganic component, combined with poly(3-hexylthiophene) (P3HT) and the fullerene derivative [6,6]-phenyl-C_{61}-butyric acid methyl ester (PCBM). As noted above, this ternary blend has shown excellent performance when used as an active layer in NIR photodiodes.[4] To understand the role of each component in the heterojunction, we studied the photoluminescence dynamics in the visible and near-infrared-spectral ranges for optical transitions in the P3HT and NCs spectra, respectively.

In the ternary blend we observed a reduction of PL intensity and decay time both for the P3HT and the NCs, as compared to the binary reference blends. Both effects are attributed to charge-transfer processes; excitations in P3HT result in an electron transfer towards PbS and PCBM, whereas excitation in the PbS-NCs provides electron transfer towards PCBM and hole transfer towards P3HT. The improved charge separation in the ternary blend is caused by hole transfer occurring between the PbS-NCs and P3HT. This process depletes the long-lived hole population established after the electron transfer from the NCs to the fullerene, and in this way boosts the excitonic splitting.

Dr. D. Jarzab, K. Szendrei, Prof. M. A. Loi
Zernike Institute for Advanced Materials
University of Groningen
Nijenborgh 4, Groningen, 9747 AG, The Netherlands
E-mail: M.A.Loi@rug.nl
M. Yarema, S. Pichler, Prof. W. Heiss
Institute for Semiconductor and Solid State Physics
University of Linz
Altenbergerstr.69, Linz, 4040, Austria

DOI: 10.1002/adfm.201001999

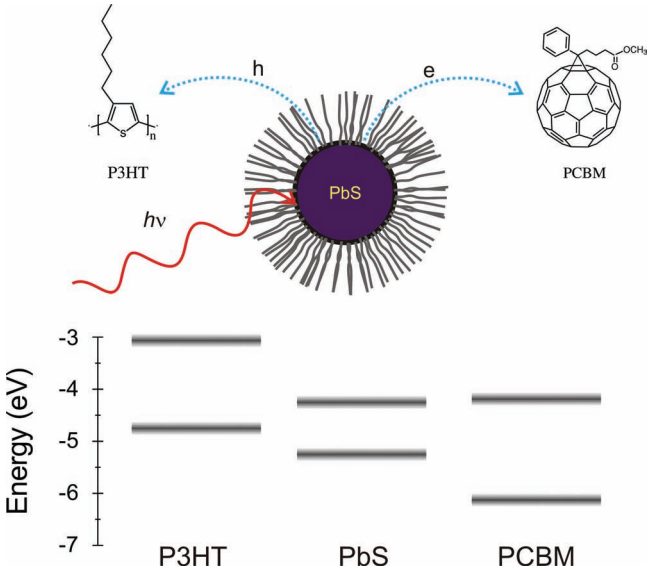

Figure 1. Chemical structure of P3HT and PCBM, and cartoon of the PbS-NCs with ligands; lower part: schematic energy-level diagram of P3HT, PCBM, and PbS-NCs.

2. Results and Discussion

Figure 1 shows the chemical structure and the schematic energy-level diagrams of PbS-NCs, P3HT, and PCBM. PbS-NCs are semiconducting particles that show NIR sensitivity, and their absorption edge is tunable between 800–1800 nm. The P3HT:PCBM blend is a well-known active medium for organic solar cells.[14,15] The blend shows good hole and electron mobility;[16,17] however, absorbs only up to 650 nm.[18] The incorporation of PbS-NCs into P3HT:PCBM heterojunctions results in an expansion of the absorption up to the near-infrared with an edge that depends upon the NCs' size, with preservation of ambipolar transport.[4]

The schematic energy-level diagram of the ternary blend (Figure 1) suggests that different processes can occur depending on the excitation energy. When excitons are formed in the PbS-NCs, it is expected that the electrons will be transferred to PCBM and the holes to P3HT. When excitations are generated in P3HT, we can predict from the energy levels that an electron transfer will occur towards PbS and/or PCBM. However, the energy levels reported in Figure 1 are rough estimates (in particular in the case of the NCs),[19–21] and the described landscape, although possible, was not demonstrated.

Steady-state and time-resolved PL are useful tools for learning more about the processes occurring between the blend components. The normalized visible-PL of the drop-cast thin films of neat P3HT, PbS:P3HT, P3HT:PCBM, and PbS:P3HT:PCBM blends are reported in **Figure 2**a. All blends display similar features which derive from P3HT. The PL behavior is characterized by three vibronic peaks centered at ~660, ~682, and ~709 nm with a shoulder at ~805 nm. Only the PL of neat P3HT film shows a slightly different spectral shape, with partial reduction of the 0–0 vibronic transition, most likely because of self-absorption of the emitted light due to the large layer thickness of the P3HT thin-film layer.[22] The PL behaviors of all three blends

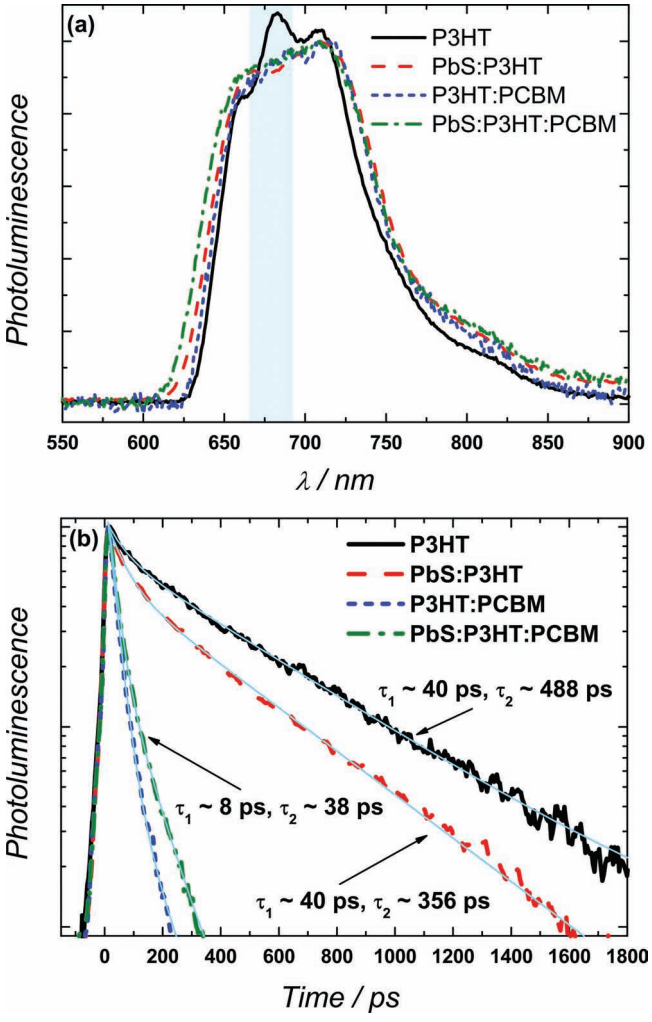

Figure 2. a) Normalized visible PL spectra and b) dynamics detected at ~675 nm and fits of P3HT, PbS:P3HT, P3HT:PCBM and PbS:P3HT:PCBM drop-cast films. The thin lines in (b) are the fitting curves.

show no significant changes in spectral shape and peak energy, but there is a substantial difference in the overall photoluminescence intensity. In particular, the ternary-blend PL displays a pronounced quenching with respect to the photoluminescence of the neat polymer and the PbS:P3HT blend. However, due to the different thickness of the film it is not possible to compare the PL intensities directly. This problem is overcome by studying the dynamics of the PL. The PL decays detected at ~660 nm, which correspond to the 0–0 vibronic transition of P3HT for all samples, are shown in Figure 2b. All decay traces are biexponential. The neat P3HT film displays the slowest decay, fitted with time constants τ_1~40 ps and τ_2~488 ps. The blend composed of P3HT and NCs shows a reduction of the long time constant of ~132 ps, and the PL decay can be fitted with τ_1~40 ps and τ_2~356 ps. The reduced PL-decay time in the PbS:P3HT blend indicates the occurrence of a charge transfer from the excited P3HT to the NCs, which is probably an electron transfer (see Figure 1). In the case of the ternary blend, the decrease of PL life time is even more pronounced; the PL decay of the PbS:P3HT:PCBM

thin film can be modeled using τ_1~8 ps and τ_2~36 ps. These time constants are comparable to the values obtained for the P3HT:PCBM thin film (τ_1~6 ps and τ_2~34 ps) due to the excitation of P3HT and the subsequent electron transfer to PCBM, which indicates a similar electron-transfer efficiency.

At this point it is very important to study what happens to the photoluminescence in the near infrared. The spectra measured for the drop-cast films of PbS, PbS:P3HT, PbS:PCBM, and PbS:P3HT:PCBM are shown in **Figure 3**a. The PL of PbS-NCs is characterized by a Gaussian-shaped band centered at ~1006 nm, with a full width at half maximum (FWHM) of ~100 nm. The PL spectrum of the PbS:P3HT blend is blue-shifted ~23 nm with respect to the PbS thin film. This spectrum can be also described by a Gaussian function with the maximum at ~983 nm and FWHM of ~124 nm. The normalized PL spectra of the PbS:PCBM and PbS:P3HT:PCBM blends overlap completely. As previously, in this case, the PL band can be described by a Gaussian function blue-shifted with respect to that of the neat PbS crystals by ~70 nm. The spectrum of this blend, as that of PbS:P3HT, shows a shoulder at ~860 nm that originates from the emission tail of P3HT and/or PCBM not cut by the low-pass filter. The large blue-shift observed in the blends, compared to the pristine NCs films, can be ascribed both to the variation of the dielectric constant of the medium (ε of PCBM is ~3.9,[17] P3HT is ~3,[23] PbS is ~17[24]) and also to the charge transfer that results in emission from higher-lying electronic states. By taking into account the different shift detected for the PbS:P3HT blend with respect to the ternary blend, we can infer a less effective charge-transfer for the first sample.

The NIR PL dynamics of PbS-NCs, PbS:P3HT, PbS:PCBM, and PbS:P3HT:PCBM thin films are reported in Figure 3b and c. The PL decays were detected at ~1006 nm, corresponding to the maximum PL intensity of neat PbS-NCs film, and no considerable difference was detected at other wavelengths. The PL of the PbS-NC thin film has a monoexponential decay with a time constant of ~200 ns. By blending the NCs with P3HT we observed a biexponential lifetime with the first decay constant τ_1≈7 ns and the second τ_2≈154 ns. The amplitude of these two time components shows wavelength dependence; at shorter wavelengths the fast component is more pronounced, while at longer wavelengths the slow component is dominant (see Figure S1 in the Supporting Information). Despite the observed decrease of the decay time, which can be interpreted as hole transfer from excited PbS-NCs to P3HT, the magnitude of the lifetime reduction (200 ns → 154 ns) shows the low efficiency of the process. The negligible efficiency is also reflected in the poor external quantum efficiency (EQE≈0.2%) of the photodiode that uses the same binary blend as the active layer.[4]

The NCs PL in the PbS:PCBM film is reduced from hundreds of nanoseconds to hundreds of picoseconds, and the decay is monoexponential with a time constant τ≈898 ps (Figure 3c). This is the signature of the efficient, ultrafast electron transfer from the NCs to the fullerene molecules, as we have previously reported.[3] It is noteworthy that in the ternary blend we observed a further reduction of the dynamics of the NCs emission with a lifetime of τ≈65 ps. This lifetime corresponds to a rate that is more than one order of magnitude faster than that of the PbS:PCBM blend and four orders of magnitude faster than that of the neat PbS-NCs film.

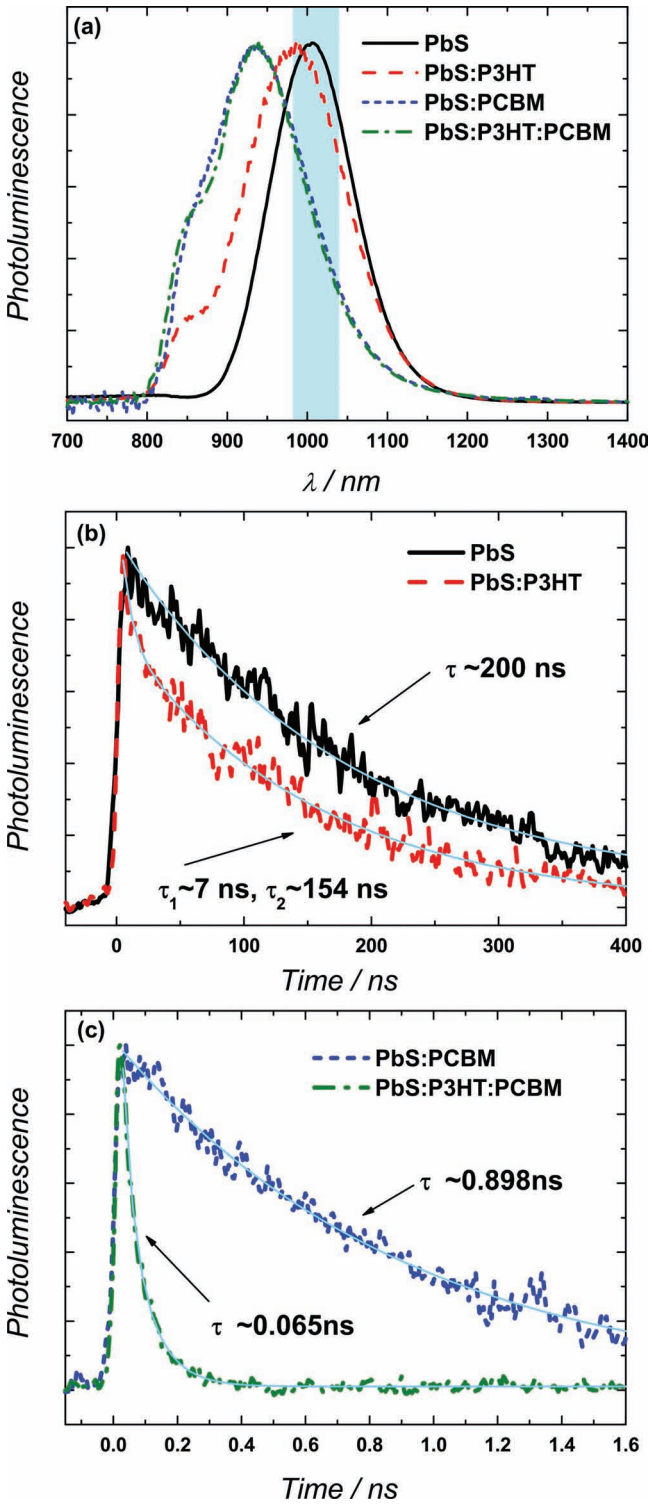

Figure 3. a) Normalized NIR photoluminescence spectra and b) dynamics detected at ~1006 nm of PbS-NCs, PbS:P3HT and c) PbS:PCBM, PbS:P3HT:PCBM drop-cast films. The blue band in panel (a) indicates the wavelength over which the dynamic traces are integrated. The thin lines are fitting curves.

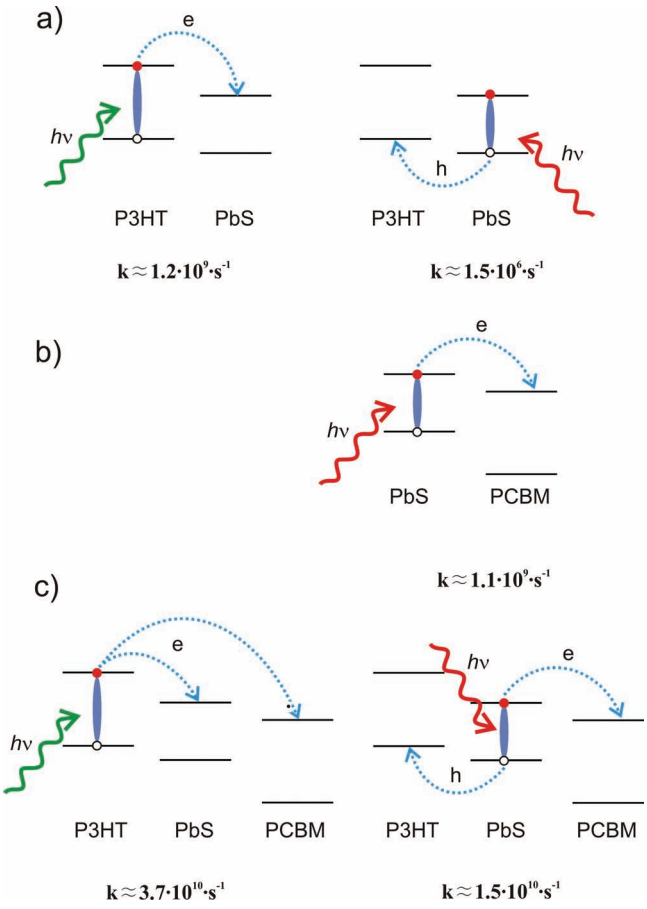

Figure 4. Schematic of the excitation and charge-transfer pathways in: a) PbS:P3HT blend, b) PbS:PCBM blend, and c) PbS:P3HT:PCBM blend. For (c) the transfer rates take into account the sum of the process indicated by the arrow.

Due to the quite complicated landscape resulting from the experiments, a schematic summary of the excitation and charge-transfer pathways is depicted in **Figure 4**. To estimate the efficiency of the charge-transfer process we calculated its rate: $k = (1/\tau_{BH} - 1/\tau_{ref})$, where τ_{BH} and τ_{ref} are the PL decay time of the blend and of the neat reference sample, respectively. Figure 4a and b illustrate the possible excitations for the binary blend both with excitation in the visible (P3HT) and in the infrared regions (NCs); the transfer rate of each process is indicated. Figure 4c reports excitation processes and transfer rates for the ternary blends.

The elevated transfer rate of $1.5 \cdot 10^{10} \cdot s^{-1}$ for the ternary blend correlates with the high efficiency of the photodiodes made with this active layer.[4] This finding highlights why a fuller understanding of the excitation dynamics of the ternary blend is extremely relevant. It is important to note that the ternary blend shows an order-of-magnitude higher transfer rate than the blend composed of PbS and PCBM. This difference cannot be justified by the opening of a second transfer path towards P3HT; in fact, this process might eventually account for a rate that is $(1.5 \cdot 10^{6} \cdot s^{-1})$ four orders of magnitude smaller than the rate of the ternary blend. Recently, we described that in the PbS:PCBM blends the holes remain trapped in the PbS-NCs after electron transfer.[3] However, in the case of the ternary blend, the hole population does not accumulate because it can be effectively transferred to P3HT. We suggest that the depletion of hole population in the NCs allows the regeneration of the exciton population, which is then available to take part in the photoinduced electron-transfer process. The presence of both P3HT and PCBM not only enables ambipolar transport in devices, but also facilitates charge extraction from the PbS-NCs.

3. Conclusions

Insight into the working mechanism of hybrid blends used for efficient near-infrared photodiodes was obtained by time-resolved photoluminescence studies. We compared the PL behavior of the ternary PbS:P3HT:PCBM blend and the binary PbS:P3HT, PbS:PCBM, and P3HT:PCBM blends with the PL of the pristine PbS-NCs and P3HT. In the ternary blend the efficiency of the charge transfer is significantly enhanced over that of the PbS:P3HT and PbS:PCBM blends, which indicates that both hole and electron transfer from excited NCs to the polymer and fullerene occur in the ternary blend. Hole transfer towards P3HT determines the equilibration of their population in the NCs after the electron transfer towards PCBM, which thereby allows their re-excitation and new charge transfer.

4. Experimental Section

Materials: Oleic-acid-capped PbS-NCs were synthesized as reported in ref. [25]. The study used PbS-NCs with diameters of 3.4 nm, which showed an absorption maximum at ~870 nm, with a highest occupied molecular orbital (HOMO) level of approximately –5.1 eV and a lowest unoccupied molecular orbital (LUMO) level of approximately –3.7 eV.[19] PCBM was obtained from Solenne Bv. P3HT with regioregularity of 98.5% was purchased from Rieke Metals. The absorption spectra of both organic systems are reported elsewhere.[18]

Sample Fabrication: Thin films of PbS, P3HT, PbS:P3HT, PbS:PCBM, P3HT:PCBM, and PbS:P3HT:PCBM were drop-cast onto quartz substrate from 5mg mL^{-1} chlorobenzene solution. The solutions were prepared in nitrogen atmosphere. The weight ratios of the blended components were: 1:1 for PbS:P3HT; 1:1 for PbS:PCBM; 1:1 for P3HT:PCBM; and 1:1:1 for PbS:P3HT:PCBM. Prior to processing, the substrates were cleaned with a standard wet-cleaning procedure, which combined ultrasonic cleaning in acetone and isopropanol.

Spectroscopy: For steady-state and time-resolved PL measurements the samples were excited at ~380 nm by the second harmonic of a mode-locked Ti:sapphire laser delivering pulses of 150 fs. To vary the repetition frequency of the exciting pulse an optical pulse selector was used. The time-resolved PL signal was recorded with two Hamamatsu streak cameras, one with a photocathode sensitive in the visible, the other in the near-infrared spectral range. Depending on the PL lifetime, the streak cameras were used in synchroscan or in single-sweep mode. All time-resolved measurements were carried out at room temperature. The steady-state PL spectra were detected in the visible range with a Si-CCD from Hamamatsu and in the near-infrared with an InGaAs detector from Andor. The PL spectra were corrected for the spectral response of the set-up. The traces of the PL decay time were integrated in a spectral region of about 20 nm, at the 0–0 excitonic transition in the visible, and at ~1006 nm, (corresponding to the excitonic peak of neat PbS-NCs). All samples, both in the visible and in the NIR regions, showed no considerable difference at other wavelengths. Samples containing PbS were also excited at 760 nm showing no significant difference with respect to the higher energy excitation.

All decays were fitted with the function:

$$I_{PL}(t) = \sum_i A_i \cdot \exp\left(-\frac{t}{\tau_i}\right)$$

where A_i, and τ_i are fitting parameters; $i = 1$ for monoexponential decay and $i = 2$ for biexponential decay.

All samples were measured in several locations; the variations in the results of the time-resolved PL measurements did not exceed the resolution of the instrument.

Supporting Information

Supporting Information is available from the Wiley Online Library or from the author.

Acknowledgements

Financial support from the European Commission through the Human Potential Programs (RTN Nanomatch, Contract No. MRTN-CT-2006–035884) and from the Austrian Science Fund FWF (Project SFB IR_ON) is gratefully acknowledged.

Received: September 22, 2010
Revised: January 7, 2011
Published online: April 12, 2011

[1] W. U. Huynh, J. J. Dittmer, A. P. Alivisatos, *Science* **2002**, *295*, 2425.
[2] N. Tessler, V. Medvedev, M. Kazes, S. Kan, U. Banin, *Science* **2002**, *295*, 1506.
[3] K. Szendrei, F. Cordella, M. V. Kovalenko, M. Böberl, G. Hesser, M. Yarema, D. Jarzab, O. V. Mikhnenko, A. Gocalinska, M. Saba, F. Quochi, A. Mura, G. Bongiovanni, P. W. M. Blom, W. Heiss, M. A. Loi, *Adv. Mater.* **2009**, *21*, 683.
[4] T. Rauch, M. Boberl, S. F. Tedde, J. Furst, M. V. Kovalenko, G. Hesser, U. Lemmer, W. Heiss, O. Hayden, *Nat. Photon.* **2009**, *3*, 332.
[5] B. O. Dabbousi, M. G. Bawendi, O. Onitsuka, M. F. Rubner, *Appl. Phys. Lett.* **1995**, *66*, 1316.
[6] S. A. McDonald, G. Konstantatos, S. Zhang, P. W. Cyr, E. J. D. Klem, L. Levina, E. H. Sargent, *Nat Mater* **2005**, *4*, 138.
[7] G. Konstantatos, I. Howard, A. Fischer, S. Hoogland, J. Clifford, E. Klem, L. Levina, E. H. Sargent, *Nature* **2006**, *442*, 180.
[8] Y. Zhou, M. Eck, M. Krüger, *Energy Environ. Sci.* **2010**, *3*, 1851.
[9] G. Cheng, M. Mazzeo, A. Rizzo, Y. Li, Y. Duan, G. Gigli, *Appl. Phys. Lett.* **2009**, *94*, 243506.
[10] M. Park, B. D. Chin, J. Yu, M. Chun, S. Han, *J. Ind. Eng. Chem.* **2008**, *14*, 382–386.
[11] A. J. Morfa, K. L. Rowlen, T. H. Reilly, M. J. Romero, J. van de Lagemaat, *Appl. Phys. Lett.* **2008**, *92*, 013504.
[12] B. V. K. Naidu, J. S. Park, S. C. Kim, S. Park, E. Lee, K. Yoon, S. Joon Lee, J. Wook Lee, Y. Gal, S. Jin, *Sol. Energy Mater. Sol. Cells* **2008**, *92*, 397.
[13] J. N. de Freitas, I. R. Grova, L. C. Akcelrud, E. Arici, N. S. Sariciftci, A. F. Nogueira, *J. Mater. Chem.* **2010**, *20*, 4845.
[14] Y. Kim, S. Cook, S. M. Tuladhar, S. A. Choulis, J. Nelson, J. R. Durrant, D. D. C. Bradley, M. Giles, I. McCulloch, C. Ha, M. Ree, *Nat. Mater.* **2006**, *5*, 197.
[15] J. Y. Kim, S. Kim, H. Lee, K. Lee, W. Ma, X. Gong, A. Heeger, *Adv. Mater.* **2006**, *18*, 572.
[16] V. D. Mihailetchi, H. Xie, B. de Boer, L. M. Popescu, J. C. Hummelen, P. W. M. Blom, L. J. A. Koster, *Appl. Phys. Lett.* **2006**, *89*, 012107.
[17] V. Mihailetchi, J. V. Duren, P. Blom, J. Hummelen, R. Janssen, J. Kroon, M. Rispens, W. Verhees, M. Wienk, *Adv. Funct. Mater.* **2003**, *13*, 43.
[18] D. Jarzab, F. Cordella, M. Lenes, F. B. Kooistra, P. W. M. Blom, J. C. Hummelen, M. A. Loi, *J. Phys. Chem. B* **2009**, *113*, 16513.
[19] B. Hyun, Y. Zhong, A. C. Bartnik, L. Sun, H. D. Abruña, F. W. Wise, J. D. Goodreau, J. R. Matthews, T. M. Leslie, N. F. Borrelli, *ACS Nano* **2008**, *2*, 2206.
[20] Z. Hens, D. Vanmaekelbergh, E. J. A. J. Stoffels, H. van Kempen, *Phys. Rev. Lett.* **2002**, *88*, 236803.
[21] F. W. Wise, *Acc. Chem. Res.* **2000**, *33*, 773.
[22] E. Tekin, H. Wijlaars, E. Holder, D. A. M. Egbe, U. S. Schubert, *J. Mater. Chem.* **2006**, *16*, 4294.
[23] J. Szmytkowski, *Chem. Phys. Lett.* **2009**, *470*, 123.
[24] L. Cademartiri, J. Bertolotti, R. Sapienza, D. S. Wiersma, G. von Freymann, G. A. Ozin, *J. Phys. Chem. B* **2006**, *110*, 671.
[25] M. Hines, G. Scholes, *Adv. Mater.* **2003**, *15*, 1844.